

PATTERNS OF BRAIN GROWTH IN ONE FGFR2 MOUSE MODEL FOR APERT SYNDROME

Jordan Austin¹, Cheryl A. Hill¹, Cortagia Gant¹, Joan T. Richtsmeier², Christopher Percival³, Neus Martinez-Abadias², Yingli Wang³, Ethylin W. Jabs³, Thomas Neuberger⁴, and Kristina Aldridge¹

¹Department of Pathology & Anatomical Sciences University of Missouri-School of Medicine, ²Department of Anthropology Pennsylvania State University, ³Department of Genetics and Genomic Sciences Mount Sinai School of Medicine, ⁴Huck Institutes of the Life Sciences, Pennsylvania State University, Hershey, Pennsylvania

INTRODUCTION

Apert syndrome is a disorder associated with craniosynostosis resulting from one of two mutations in Fibroblast Growth Factor Receptor 2 (FGFR2). Individuals with Apert syndrome demonstrate brain dysmorphology, often associated with cognitive deficits. In this study, micro magnetic resonance images of the brain of $FGFR2^{+/P253R}$ mice and their wildtype littermates were acquired at two ages, P0 (newborn) and P2 (two days old). Fifteen landmarks on the brain surface were collected to compare growth patterns in the morphological phenotypes of the brain. Patterns of growth between P0 and P2 were defined for both the mutant and wildtype mice. These growth patterns were then compared between the mutant and wildtype groups. In general, mice with the $FGFR2^{+/P253R}$ mutation demonstrate a greater magnitude of growth of the brain compared to wildtype littermates between P0 and P2. Differences in growth between mutants and wildtypes are particularly evident in the width of the cerebrum, while growth of the cerebellum is more similar in the two groups of mice. This differential growth is similar to brain dysmorphologies observed in individuals with Apert syndrome and may underlie the cognitive deficits associated with this disorder.

MATERIALS AND METHODS

Generation of targeting construct and mutant mice

The Apert $Fgfr2^{+/P253R}$ mice were generated on a C57BL/6J background at Mount Sinai School of Medicine (Wang et al. 2005; Sun et al. 2009). Mice were sacrificed at P0 (i.e., day of birth) and P2 (2 days after birth) by inhalation anesthetics, fixed, and heads perfused in 4% paraformaldehyde. Genotyping of tail DNA was carried out by PCR analysis. Our sample included: $Fgfr2^{+/P253R}$ mice sacrificed at P0 and P2 and their wildtype littermates, also sacrificed at P0 and P2.

Imaging protocols

Magnetic resonance microscopic (MRM) images were acquired on a vertical 14.1 Tesla Varian (Varianninc., Palo Alto, CA) imaging system at the High Field Magnetic Resonance Facility at the Pennsylvania State University. Images up to an isotropic resolution of 40 μ m were acquired. MRM protocols described previously (Aldridge et al. 2010).

Phenotypic analysis

3D reconstructions of MRM images were used to assess gross morphology of the brain, including overall morphology, symmetry, corpus callosum appearance, and ventriculomegaly.

Fifteen 3D biological landmarks were collected from the MRM images, to assess brain size, quantitative morphology, and average growth from P0 to P2, shown in Figure 1. Precision of landmark data collection was evaluated following previously described methods (Aldridge et al. 2007). We quantitatively assessed brain morphology using Euclidean distance matrix analysis.

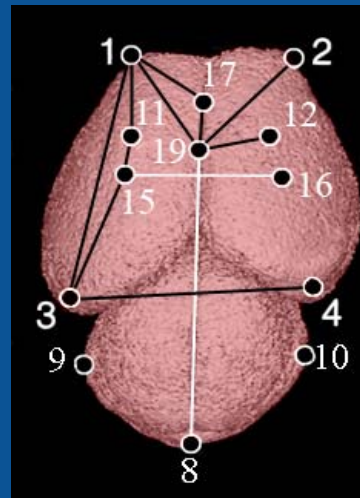


Figure 2: Lines showing linear distances between landmarks as an average of growth compared between P0 and P2. Black lines show an increased distance, and white show a decreased distance.

RESULTS

The Apert $Fgfr2^{+/P253R}$ mice showed an increased magnitude of growth between P0 and P2 as compared to the wildtype mice, particularly in the width of the cerebrum (Figure 2). The increased magnitude of growth was seen most clearly in the anterior aspect of the frontal lobe, as well as between the genu and splenium of the corpus callosum. The increased growth was also seen in the superolateral points of the anterior frontal lobe. There is also a greater magnitude of growth seen in the relationship of the caudate nuclei (landmarks 11 and 12) with the anterior aspect of the frontal lobe.

Reduced growth in the mutants was seen between the splenium of the corpus callosum and the most caudal point of the cerebellar surface, suggesting a rostrocaudal decrease in the midbrain and cerebellum, as well as between the origins of the middle cerebral artery on the ventral cerebral surface, suggesting decreased width of the base of the cerebrum.

DISCUSSION

Apert syndrome and mouse models for Apert syndrome are characterized by synostosis of the coronal sutures with patency in the metopic and sagittal sutures, as well as by a host of anomalies in the CNS, particularly increased overall size, increased size of the ventricles, and corpus callosum dysmorphology (Aldridge et al. 2010). Due to the enlargement of the ventricles, structures in their immediate proximity are likely to be affected. We observe this specifically in the caudate nuclei, and the splenium and genu of the corpus callosum. This greater magnitude of growth seen in the corpus callosum represents the frequently seen dysmorphology of the corpus callosum in Apert syndrome (Aldridge et al. 2010). Increased magnitude of growth is also seen in the anterior aspects of the frontal lobe. This increase could be caused by enlargement of the lateral ventricles, due to the proximity of the caudate nucleus to the lateral ventricles. The combination of these traits could also account for the increased growth seen in the rostrocaudal length of the corpus callosum.

Reduced magnitude of growth was seen between the origins of the middle cerebral artery on the ventral surface of the cerebrum (landmarks 15 and 16). This reduction could be due to malformations of the cranial base, another trait seen in Apert syndrome (Tokumaru et al. 1996), resulting in shorter width along the ventral surface of the cerebrum.

CONCLUSION

The results of this study show a correlation between observed morphology of the mutant mice from P0 to P2 and the dysmorphologies associated with Apert syndrome. The overall growth of the mutant mice showed an increased magnitude of growth in the corpus callosum, and between the caudate nuclei and the anterior aspect of the frontal lobe. These data point to corpus callosum dysmorphology, enlargement of the ventricles, and cerebral asymmetry, all of which are malformations associated with Apert syndrome. Although, these results do not definitively point out the presence of these malformations in all individuals with Apert syndrome, an observable trend in growth among individuals with the $Fgfr2^{+/P253R}$ mutation can be identified.

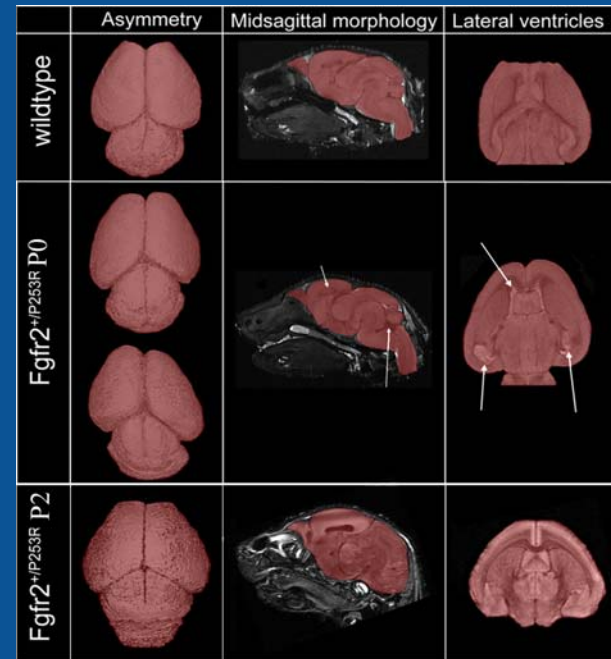


Figure 3: 3D reconstructions of dorsal surfaces (1st column), midsagittal planes (2nd column), and axial slice images (last column) of MRM data, illustrating examples of variation in brain phenotypes. Row 1: wildtype mouse. Row 2: $Fgfr2^{+/P253R}$ P0 mice with slight cerebral asymmetry (above) and severe cerebral asymmetry (below), enlarged 4th ventricle and arched corpus callosum (white arrows) and enlarged lateral ventricles (white arrows). Row 3: $Fgfr2^{+/P253R}$ P2 mice

ACKNOWLEDGEMENTS AND REFERENCES

Work supported by NIDCR R01 DE018500.

Hill CA, Reeves RH, Richtsmeier JT. 2007. Effects of aneuploidy on skull growth in a mouse model of Down syndrome. *J Anat* 210:394-405.

Tokumaru A, Barkovich A, Ciricillo S, Edwards M. 1996. Skull base and calvarial deformities: association with intracranial changes in craniofacial syndromes. *AJNR Am J Neuroradiol* 17:619-630.

Aldridge K, Reeves R, Olson L, Richtsmeier J. 2007. Differential effects of trisomy on brain shape and volume in related aneuploid mouse models. *Am J Med Genet Part A* 143A:1060-1070.

Aldridge K, Cheryl A. Hill, Jordan R. Austin, Christopher Percival, Neus Martinez-Abadias, Thomas Neuberger, Yingli Wang, Ethylin Wang Jabs, and Joan T. Richtsmeier. 2010. Brain Phenotypes in Two FGFR2 Mouse Models for Apert Syndrome. *Dev Dyn* 239:987-997.



Figure 1: Landmarks collected from MRM images of P0 and P2 mouse brains illustrated on 3-D reconstructions of the MRM images (P0 shown). A. Dorsal view B. Lateral view of right side C. Midsagittal view D. Axial slice